

In the period of evaluation, six slots have been given to the consortium. However, the fifth one has been used at the end of January so there has not been enough time for a proper processing of the data. The sixth slot is due in March. These are the reports of the four slots:

## Structure of the EndoS-Fc complex

IP: Marcelo Guerin

In order to evade host immunity, many bacteria secrete immunomodulatory enzymes. *S. pyogenes*, one of the most common human pathogens, secretes the endoglycosidases EndoS and EndoS2, which remove *N*-glycans linked to Asn297 of human IgG antibodies. EndoS hydrolyses biantennary CT *N*-glycans, while EndoS2 can also remove HM-type *N*-glycans. Both enzymes belong to the GH18 family, where we can find a subfamily of endoglycosidases with distinct substrate and *N*-glycan specificity. Unique amongst bacterial endoglycosidases, EndoS and EndoS2 are highly specific to the protein part of the substrate, hydrolyzing only *N*-glycans from antibodies. This renders antibodies incapable of eliciting host effector functions through either complement or Fc  $\gamma$  receptors (Fc $\gamma$ Rs), providing the bacteria with a survival advantage. Because antibodies are central players in many human immune responses and bridge the innate and adaptive arms of immunity, the analysis and manipulation of the enzymatic activity of EndoS and EndoS2 impacts diverse fields in biomedicine. Understanding the molecular basis of antibody-specific deglycosylation of EndoS-like enzymes is a crucial next step not only to design EndoS-like enzymes variants to antibody engineering but also to produce selective enzymes for an specific IgG isotype (IgG1-4) in order to treat a wide range of autoimmune diseases.

Strikingly, we have obtained a ca. 4.5 Å resolution reconstruction of the EndoS-IgG1(Fc) complex (**Figure 1a**). This reconstruction already discloses significant structural information about the mechanism of action of the endoglycosidase EndoS. The cryoEM structure shows that the enzyme binds preferentially to one monomer of the Fc domain of the IgG through the GH and the CBM domain (**Figure 1b**). Importantly, neither *N*-glycans of the IgG1(Fc) directly interact with the CBM, indicating that this domain is a  $\beta$ -sandwich that mediates protein-protein interaction with the CH2 domain of the Fc. Therefore, the *N*-glycan of this Fc monomer certainly needs to be flipped into the active site of the enzyme by the rotation of the Asn297 in order to be hydrolyzed (**Figure 1b**). This conformation is favoured by interaction of the CH2 domain of the Fc with the GH and CBM of the EndoS.

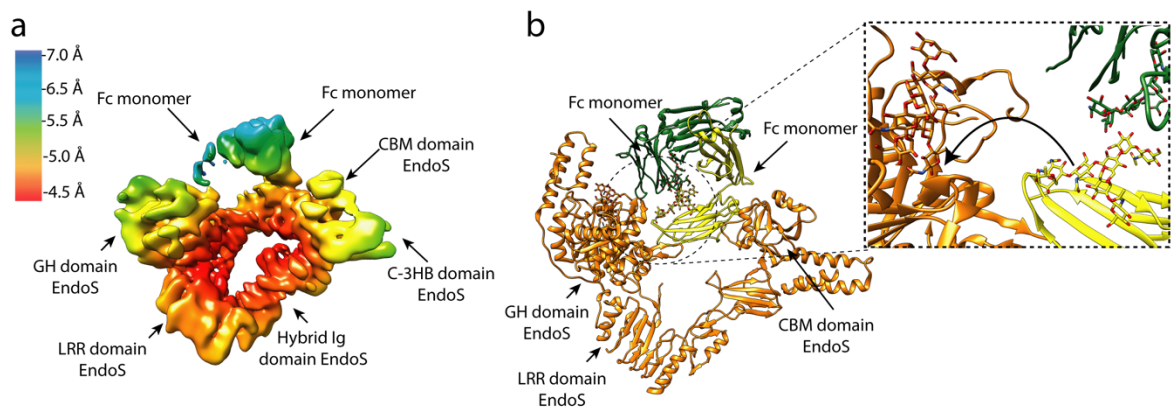


**Figure 1. a.** View of the EndoS-Fc complex single particle reconstruction at 5 Å resolution by cryo-EM **b.** 3D model of EndoS (orange) in complex with the Fc fragment, each monomer is coloured in yellow and green.

## Structure of the chaperone DnaJA2

PI: José M. Valpuesta

Hsp40s form the largest and functionally most diverse chaperone family. They are usually divided in three classes (A, B and C) considering their domain content with a high degree of structural and functional variability between and within the classes. Common to all of them is the presence of a J domain. In class A proteins, the J domain is followed by a flexible glycine/phenylalanine (G/F)-rich domain, two homologous  $\beta$  sandwich domains (CTD I and II), with a Zn<sup>2+</sup>-finger domain inserted into the first one, and a C-terminal dimerization domain. Regarding function and specificity, class A and class B are considered general cochaperones that interact with unfolded, misfolded, or aggregated proteins and transfer them to Hsp70. Although high-resolution structures of different domains of J-proteins are available, the structure of a full-length class A or class B Hsp40 has not been solved so far. This could be due to the high conformational dynamics of these multidomain Hsp40s. Class A and class B DnaJs generally assemble and function as dimers formed by inter-subunit interactions between the C-terminal dimerization domains. However, Hsp40 dimers can adopt different structures, and can also transiently assemble into higher order oligomers. We have found that class A DnaJA2 self-associates to form higher order oligomerization states which we want to structurally characterise using cryoEM. For that, we have used a DnaJA2 mutant that lacks the G/F domain (DnaAJA2  $\Delta$ G/F) and as the wt version, generates large, helical structures. DnaAJA2  $\Delta$ G/F oligomers have been formed and vitrified samples have been used to record images (Fig. 2A). The data is currently being processed, but it has already provided a preliminary 3D reconstruction at 5.5 Å resolution (Fig. 2B)

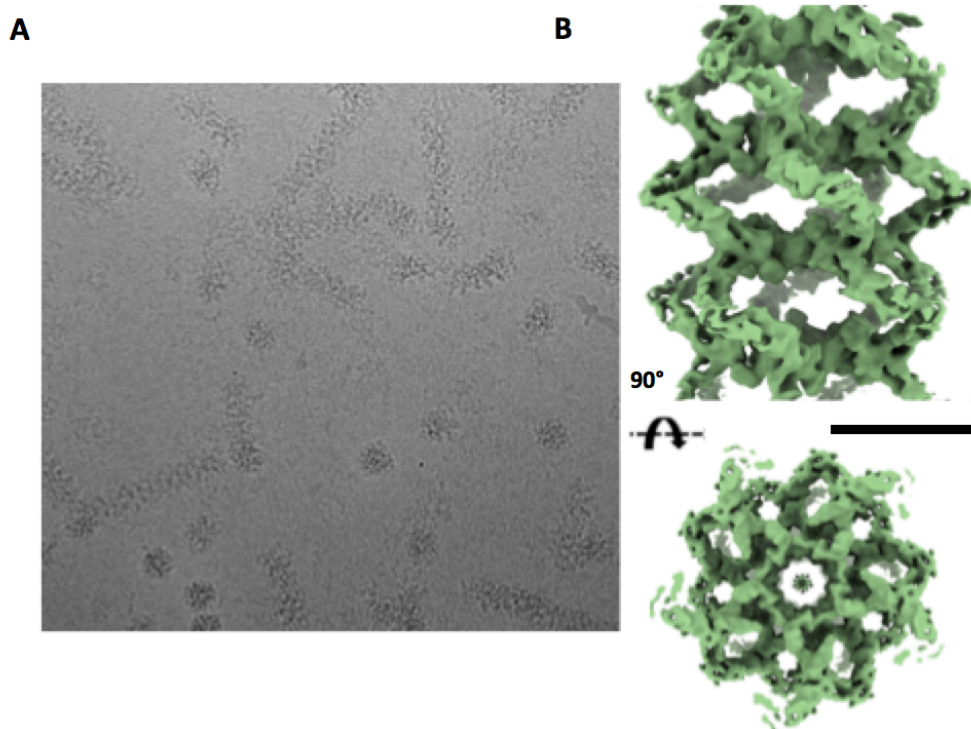
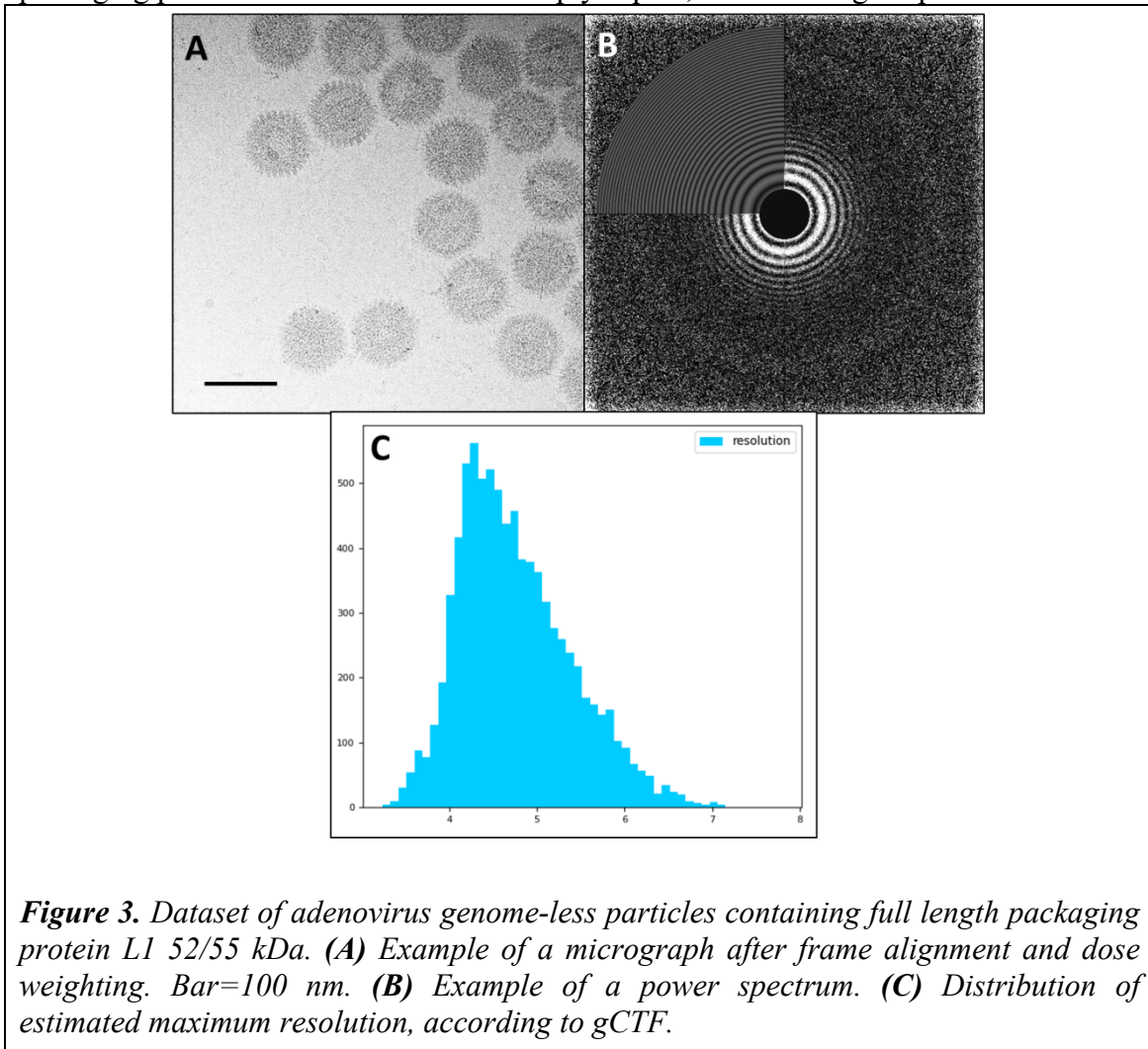


**Figure 2.** CryoEM structure of DnaJA2  $\Delta$ G/F. **A)** Representative field of a CryoEM image of DnaJA2  $\Delta$ G/F. **B)** Side and top views of the preliminary 3D reconstruction of DnaJA2  $\Delta$ G/F at 5.5 Å resolution. Bar indicates 100 Å.

## Structure of the adenovirus genome-less particles

PI: Carmen San Martín

The CSM group investigates the physical and structural principles governing complex virus assembly. As a model system they use adenovirus, a specimen of interest in both basic virology and biomedicine. Adenovirus genome packaging requires the coordinated action of at least four different proteins (L1 52/55 kDa, L4 33kDa, L4 22kDa, IVa2), some of which are only present in genome-less capsids. There are no structural data on any of these proteins, and only limited, low resolution information on their localization within the viral particle (10.1128/jvi.01453-15). Using data acquired at other facilities (eBIC), we have obtained a 3.5 Å-resolution map of an adenovirus genome-less capsid containing partially mature L1 52/55 kDa protein. At our mx2263 ESRF data collection session of 07/12/20, we imaged adenovirus genome-less capsids containing full length, immature L1 52/55 kDa. Data were obtained on a Titan Krios microscope using a K2 detector in counting mode at 105k magnification, with an electron dose of  $20 \text{ e}^-/\text{Å}^2$ . During the session, 8398 movies were collected, aligned and dose weighted (Fig. 3). Data processing is under way. Once a 3D map is obtained, we will compare it with the one mentioned above to obtain information on the location of packaging protein L1 52/55 kDa in the empty capsid, and its changes upon maturation.



1. Condezo *et al.*, *J Virol* **89**, 9653 (2015).

## New treatments for associated inborn errors of metabolism through allosteric regulation of phenylalanine hydroxylase revealed by Cryo-EM.

PIs: Aurora Martínez, Juan Antonio Hermoso and Rafael Fernández-Leiro

Inborn errors of metabolism (IEMs) are associated with mutations in central metabolic enzymes leading to dysfunctional dynamics and function, affecting their allosteric regulation by substrates and specific metabolites. Mutations in phenylalanine hydroxylase (PAH) cause phenylketonuria (PKU), the most common IEM in humans. This project tackles highly regulated liver enzyme PAH to fully understand its allosteric activity and control it by designing allosteric regulators. Human PAH is tetrameric and multidomain protein. This arrangement allows its complex regulation. We have recently solved the long-awaited structure of full-length human PAH using X-ray crystallography (Flydal MI *et al.* 2020 Proc Natl Acad Sci). To understand its allosteric regulation, we are studying its structure in the presence of different substrate and cofactors. In the presence of substrate, the enzyme becomes exceptionally dynamic. We resorted to cryo-EM to tackle these challenging structures, which allows studying the structure of biomolecules at near-atomic resolution while capturing multiple dynamic states. This approach has allowed us to obtain multiple structures with different substrates.

In this session, we have collected data from PAH in complex with the cofactor BH<sub>4</sub> and the non-hydrolysable substrate analogue THA to complete this study. Preliminary analysis of this complex (data from eBIC-Diamond) showed promising micrographs and 2D classes. We collected a high-quality dataset of 5363 movies using this session to increase particle count and tackle the high flexibility of this particular PAH complex. Initial analysis of the data unexpectedly showed low intact-particle count per micrograph (Fig 4A) and, unfortunately, 2D classes from initial analysis do not meet the required quality (Fig. 4B). Further stabilisation of the protein during sample preparation was necessary. Using this information, we have optimised the protocol (incubation time and substrate concentration). Preliminary data from the improved sample shows promising data (Fig1B). **This improvement would not have been possible without the data from this session.** We hope to collect a new dataset on this improved sample and solve this critical structure soon.

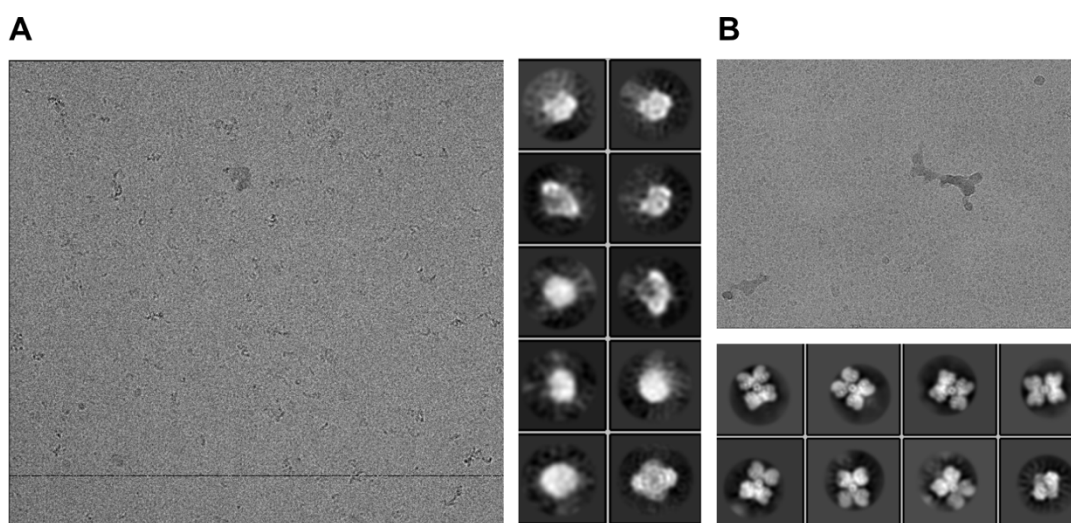


**Figure 4. Structural analysis of PAH.** (A) Representative micrograph (left) and 2D class averages (right) from 2020-08-28 dataset. (B). Preliminary data from improved sample - micrograph (up) and 2D class averages (down).

